SICE Annual Conference in Sapporo, August 4-6, 2004
Hokkaido Institute of Tecnology, Japan

High Resolution Tactile Display Using Acoustic Radiation Pressure

Takayuki Iwamoto, Daisuke Akaho and Hiroyuki Shinoda
The University of Tokyo, 7-3-1 Hongo Bunkyo-ku, Japan
{iwa,akaho,shino}@alab.t.u-tokyo.ac.jp

Abstract: We discuss the feasibility of a new tactile display using acoustic radiation pressure. We confirmed the prototype system produced 1mm diameter focal point and 0.64 gf total force. Temporal property of radiation pressure was sufficient for precise tactile stimulations. We also propose a method for scanning radiation pressure in 2-dimensional plane using a simple apparatus.

Keywords: tactile display, ultrasound, acoustic radiation pressure, phased array

1. Introduction

In recent years, various methods have been proposed to artificially produce cutaneous sensation. Except for the recent electrical nerve-stimulation method [1], the most popular method is to invoke tactile sensation by stimulating the surface of the skin mechanically. Ikei [2] developed a texture display which has fifty pins arranged in a 5-column-10-row array at a 2 mm pitch. G. Moy et al. [3] used a pneumatic method for actuating stimulators. Konyo et al. [4] developed a system using elastic gel actuators to obtain elasticity of stimulators. Pasquero and Hayward projected piezo-based tactile display with 1 mm resolution [5]. These mechanical methods are already useful to transmit a subset of tactile sensation. However, many researchers are eager for a device that can control stress field precisely on the skin with high temporal and spatial resolution as a platform for scientifically clarifying human tactile sensation, and for developing new applications of tactile information.

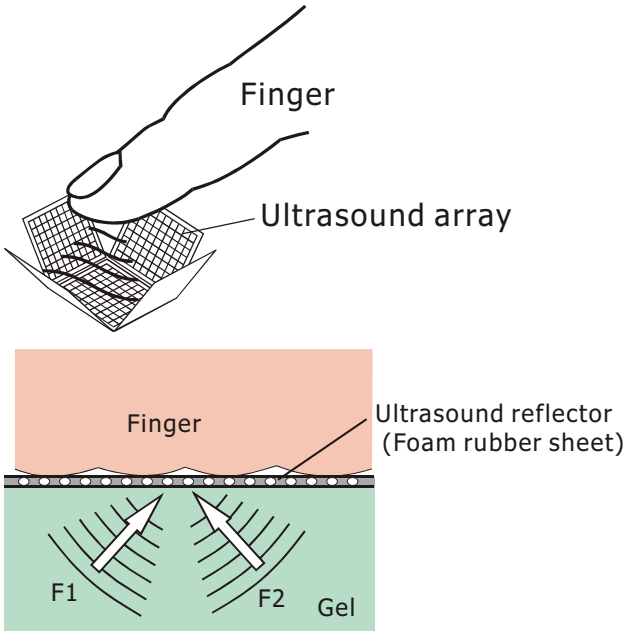

Fig. 1. Tactile display using acoustic radiation pressure

The goal of our research is realizing such a platform-device. In this paper, we examine radiation pressure generated by ultrasound as the basic tool. Previous studies [6,7] showed the relationship between the acoustic radiation pressure and tactile sensation. In these studies, they used concave transducers or acoustic lens for convergence, which generated fixed focal points. In present study, we fabricated linear phased arrays especially designed for high-power driving using PZT. If we control beam directions, pressure on the skin can be controlled with high resolution. The wave length of 3 MHz ultrasound, for example, is as small as 0.5 mm. We show the basic design and results of feasibility studies using a one-dimensional phased array of ultrasound transducers.

2. Method

Fig. 1 shows the basic principle of the tactile display using acoustic radiation pressure. Users put their fingers on an elastic gel covered with a thin ultrasound reflector. The reflector is easily realized by a thin foam rubber sheet because of the large impedance mismatching between the solid and the air. When we focus the ultrasound near the surface, radiation pressure proportional to the acoustic energy density is induced. The radiation pressure P by a vertical beam to the surface is given as

$$P = \alpha E = \alpha \frac{p^2}{\rho c^2} \tag{1}$$

where E, p, ρ and c are energy density of the sound beam near the surface, acoustic pressure, density of the sound medium, and the sound velocity, respectively. α is a constant related to the reflection property of the surface. If all the acoustic energy is absorbed on the surface, α is equal to 1, while for the surface that reflects all the sound energy, α is 2.

The sound power E carried by the beam is given as

$$E = W / c \tag{2}$$

PR0002/04/0000-1239 ¥400

where, W is power density of the transducer. The smaller the sound velocity is, the larger the radiation pressure becomes for a constant power loss. The sound velocity of air, for example, is about 340 m/s while that of water is about 1,500 m/s. However, because of the easiness in impedance matching between a PZT sound emitter and a sound medium, we chose ultrasound-conductive gel as a sound medium.

One obvious advantage of using ultrasound for tactile display is the large margin of frequency between the ultrasound and human tactile perception. If we use 5 MHz ultrasound, the frequency is 5,000 times larger than the bandwidth of tactile perception 1 kHz. Then, it is easy to scan the focused beam over an effective area. If the focused spot diameter is 1 mm, a 1 cm by 1cm area can be scanned within 1 ms even if the beam stays for 10 μ sec (50 times larger than the period of the sound) for one stimulating point.

The second advantage is the spatial resolution. If we use 3 MHz ultrasound, the wavelength is 0.5 mm in water or ultrasound-conductive gel. This means such high frequency sound can generate fine pressure pattern by radiation pressure without any fragile mechanical parts.

The third advantage is that it is free from contact problems because the device surface is elastic. When we stimulate the skin mechanically with hard pins, it is difficult to control the contact condition and contact pressure precisely. Unexpected forces arise by the movements of the user's skin. If we use radiation pressure, we can easily control the pressure on the skin instead of the displacement. We confirm these properties experimentally in the following sections.

3. Experimental setup

We fabricated linear phased array especially designed for high-power driving using PZT. The power limit is given by the maximum electrical field to maintain polarization of the PZT and the maximum temperature as the Curie temperature. In order to avoid temperature rising, the PZT pieces are attached on a thermally conductive material. The details of the apparatus are as follows.

3.1 Linear Phased Array

We used two different linear array transducer components (Nihon Dempa Kogyo Co., Ltd.). One component has 10 pieces of 1MHz PZT transducers. The width of each transducer is 0.95 mm and the length is 10 mm. The 10 transducers are arranged in a 1mm pitch. The other component consists of 30 pieces of 3 MHz PZT transducers arranged in a 0.5 mm pitch. The width of each transducer is 0.445 mm and the length is 10 mm. As for both 10 ch and 30 ch components, each piece of a PZT transducer is fixed on an aluminum bulk. Thin backing materials are attached between transducer and the aluminum bulk. An acoustic impedance matching layer is in contact with the front side of each transducer.

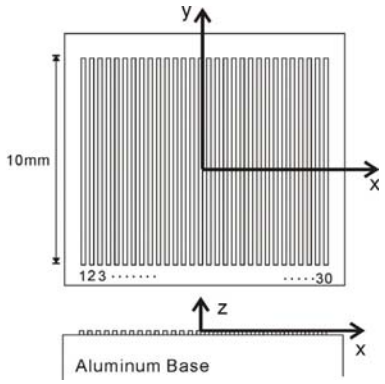

Fig. 2. Linear array transducer component (3MHz,30ch)

3.2 System

The system consists of a linear array transducer component shown in Fig.2, driving circuits, and a water bath for basic measurements. The photograph of the system is shown in Fig.3

The driving circuits include signal delay circuits implemented with 4-bit counters. The signal for each transducer is controlled so that ultrasound from each PZT transducer converge along x axis. A cylindrical acoustic lens is attached to the linear transducer components so that the ultrasound from each PZT transducer is converged on a single focal point.

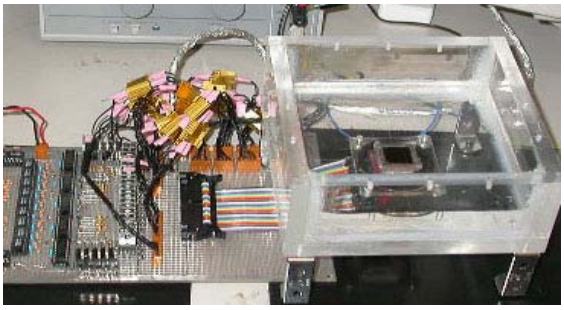

Fig. 3. Experimental setup

4. Measurement of radiation pressure

We measured acoustic radiation pressure with a point-aperture pressure sensor with bandwidth from 20 Hz to 1 kHz. We present frequency characteristics, spatial distribution of radiation pressure for a single focal point, and the relationship between instantaneous electricity and total output of radiation pressure.

Fig.4 shows a schematic drawing of the experimental setup. The pressure sensor is moved by XYZ-stage. The cross section drawing of the pressure sensor is shown in Fig.5. A pressure sensor is covered by an aluminum solid (thickness 2 mm) with a small hole of 0.5 mm in diameter at its center, while a thin elastic film (thickness 30 μ m) covers the hole. This pressure sensor was calibrated by being compared with a microphone in the air.

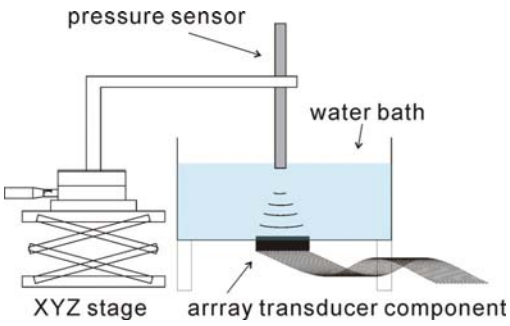

Fig. 4. Experimental setup

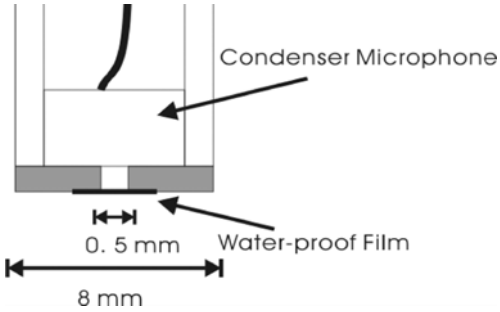

Fig. 5. Cross section drawing of the pressure sensor

4.1 Temporal characteristics

First, we present a typical waveform of the observed radiation pressure generated by a burst wave.

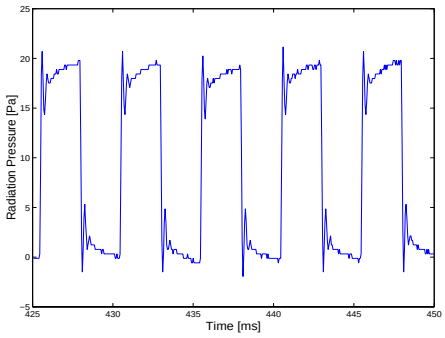

(a)

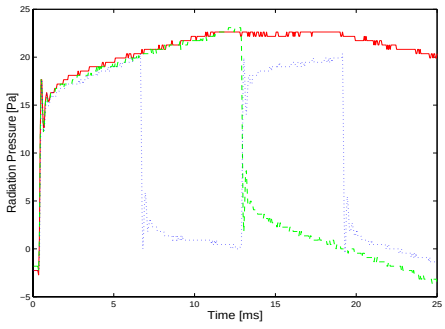

(b)

Fig. 6. Observed pressure waveforms. Radiation pressure by 200 Hz burst wave (a), and radiation pressure by 20, 40 and 80 Hz burst waves (b)

We modulated the carrier signal with period of 5 ms. Ultrasound beam was focused on a fixed focal point. The pressure waveform detected by the pressure sensor is depicted in Fig.6(a). This waveform was captured for 25 ms from 425 ms after ultrasound duration started.

The high frequency vibration at 4 kHz seen at the rise of the waveform is the resonance of the pressure sensor itself. However, the low-frequency deformation of waveform from an ideal rectangular wave (that does not depend on the modulation frequency as Fig.6(b) shows) is caused by the dynamics of the ultrasound medium. The radiation pressure is induced not only on a reflector surface but also throughout the beam-path. Then the sound medium also moves which affect the pressure on the surface.

4.2 Frequency characteristics

As we show in 4.1, radiation pressure rapidly increases up to desired pressure while the low-frequency deformation is observed in its waveform. In order to quantify its temporal characteristics, we show the gain and phase frequency response of radiation pressure.

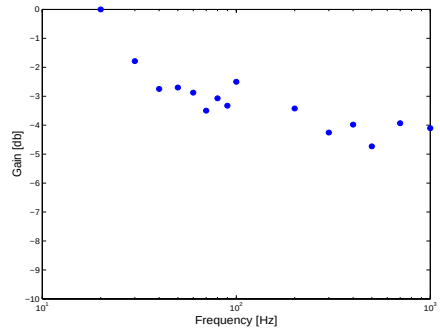

(a)

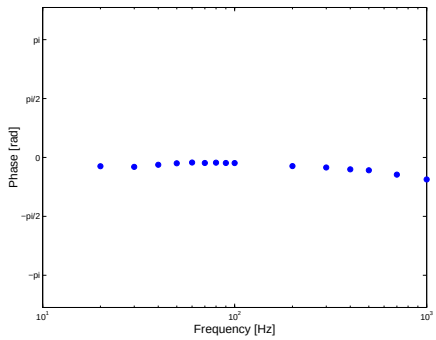

(b)

Fig.7. Frequency characteristics of radiation pressure produced using 1 MHz, 10 ch linear array component (a) gain (b) phase

1 MHz, 10 ch transducer component was used. The 1 MHz driving signal for each channel was modulated by burst wave ranging from 20 Hz to 1 kHz. Ultrasound beam is focused on a fixed focal point. The pressure sensor was fixed at the focal point. Fig.7 shows the gain-frequency characteristic of radiation pressure. The gain is determined as

$$20\log_{10}\frac{G_f}{G_{20}} \quad (4)$$

where Gf is the gain at frequency f Hz. The frequency characteristics curve is not perfectly flat, but the fluctuation of the gain was within 5 dB from 30 Hz to 1 kHz.

4.3 Spatial distribution for a single focal point

In this experiment we investigated the spatial distribution of radiation pressure for a single focal point. Ultrasound beam was focused on a fixed focal point just above the device center at 30 mm from the device surface. Here we define x-y coordinates on the surface so that the y is along the one-dimensional PZT piece. We measured radiation pressure from -2.5 mm to 2.5 mm for both x and y.

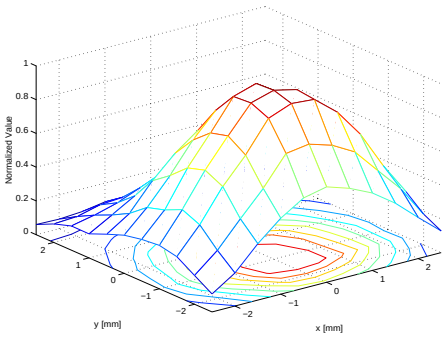

(a)

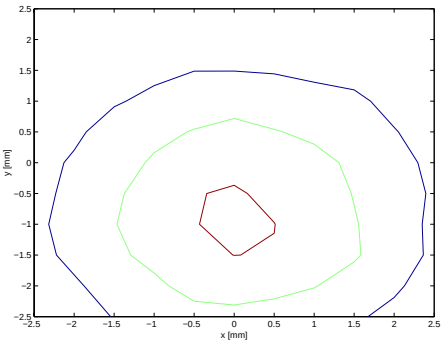

(b)

Fig.10. Spatial distribution of radiation pressure for 1 MHz 10 ch transducer component. (a) 3-D plot (b) contour plot; brown, green, blue lines are for 75%, 50%, 25% of the maximum intensity, respectively.

The results are shown in Fig.10 and Fig.11. (a) is a 3-D plot of the pressure distribution. Z-axis in (a) is the pressure obtained at each point normalized by the pressure at the origin. (b) is a contour plot of the data.

We define the focal point as the area in which the obtained pressure is higher than the half value of the pressure at the peak. Then the width of the focal point along the x axis is estimated as 2.5 mm for 1 MHz transducer and 1 mm for 3 MHz transducer.

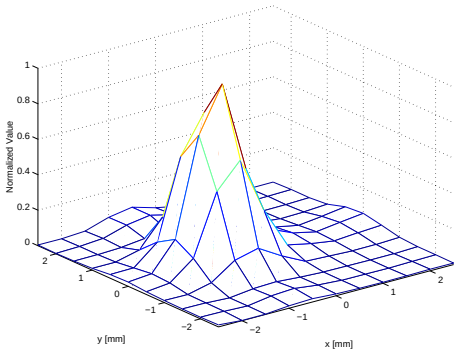

(a)

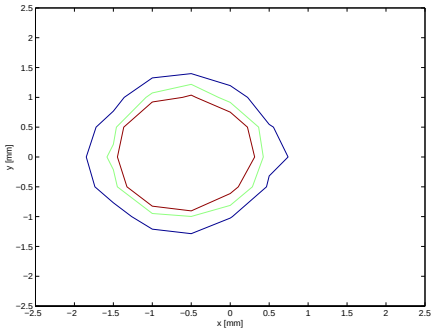

(b)

Fig.11. Spatial distribution of radiation pressure for 3 MHz 30 ch transducer component. (a) 3-D plot (b) contour plot; brown, green, blue lines are for 75%, 50%, 25% of the maximum intensity, respectively.

Next we swung the beam along the linear array (in x direction). Fig.12 shows the observed pressure distributions for the electrically moved focal point produced by 3 MHz, 30 ch transducer component.

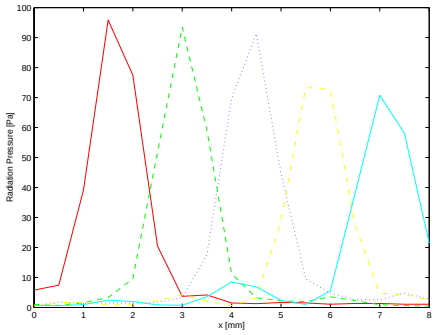

Fig.12. Spatial pressure distributions for swung beams: red x_f =1.5 mm, green x_f =3.0 mm, blue x_f =4.5 mm, yellow x_f =6.0 mm, cyan x_f =7.5 mm

4.4 Radiation pressure vs. Electricity

As we described in chapter 2, intensity of radiation pressure is supposed to be proportional to the energy density of the sound field. We investigated the relationship between the input energy and the resulting total force from radiating surface quantitatively.

The result is acquired using 3 MHz, 30 ch transducer component. The graph shows that the induced radiation pressure is relatively proportional to the input power if the input power is lower than about 45 W. But the resulting total force reaches a saturation point if the input power is higher than 60 W. The limit of the resulting total force is 0.64 gf.

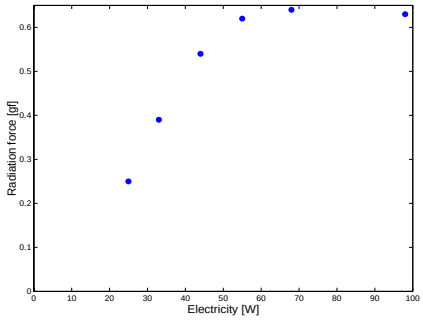

Fig.13. Input electricity vs. radiation pressure (3MHz,30ch)

4.5 2-dimensional scanning

In previous sections, we investigated the general features of acoustic radiation pressure produced by using a one-dimensional array with an acoustic lens.

Our tactile display can precisely generate various kinds of tactile stimulations even if the array transducer component is only one-dimensional array. But, in order to carry out some kinds of psychophysics experiments (for example, scanning objects on the skin surface along diagonal directions to investigate how humans perceive the directions of moving objects [8]), it is necessary that the system can control the position of the focal point on 2-dimensional surface.

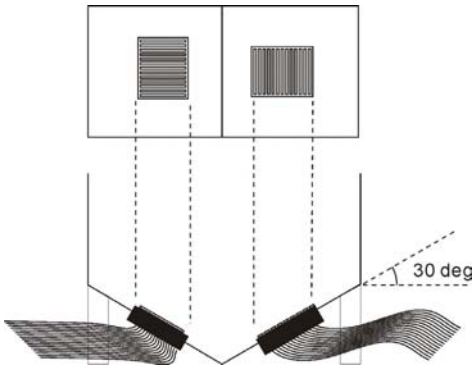

Fig.14. Schematic drawing of an experimental setup for 2-D scanning

A simple and direct way to implement 2-dimensional scanning function is to fabricate 2-dimensional array transducer component [9]. Assume the total area of the radiating surface is 10 cm^2, then the number of required PZT pieces (3MHz, arranged in a 0.5mm pitch) is about 4000. It is quite difficult to wire and drive 4000 pieces separately. In addition, fabricating such a specialized device would be quite expensive.

Compared with fabricating a complicated, expensive 2-dimensional array, it is much easier to arrange several 1-dimensional array components so that ultrasound from each transducer converges within a particular area.

We tested such method with a system as follows. Two 1-dimensional array transducer components are attached at the bottom of a water bath. (Fig.14) The bottoms of the water bath are inclined at 30 degree. The orientation of the PZT pieces of one array transducer component and that of another array transducer component are orthogonal.

Fig.15 shows the spatial distribution of acoustic radiation pressure produced by two array transducer components. Because the alignment of two arrays was not so accurate, the spatial distribution is not symmetry.

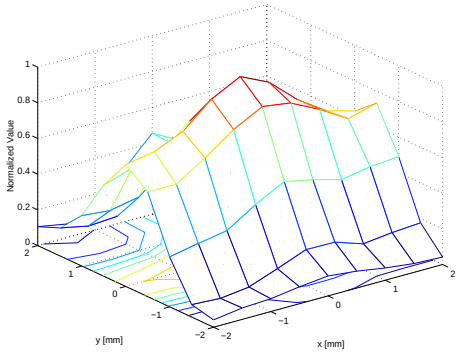

(a)

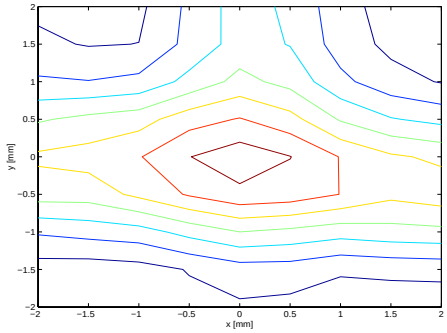

(b)

Fig.15. Spatial distribution of radiation pressure for two transducer components arranged as in Fig.14. (a) 3-D plot (b) contour plot

5. Summary

The prototype system created 1mm focal width. This sharpness is sufficient for a finger pad tactile display compared to two point discrimination [10]. Smaller spot would be useful to investigate more microscopic phenomenon, for example, the relationship between fingerprint and the direction of stress, microscopic stick-slip, etc. But producing smaller spot requires higher frequency ultrasound, which introduces much more complicated transducers and driving circuits, as a trade-off.

As to temporal resolution, the advantage of our system is its reaction time to the control signals. As seen in Fig.6, radiation pressure rapidly rose (faster than at least 1 ms)

which was independent of the burst frequency. This property is quite useful for precisely stimulating RAI and RAII mechanoreceptors which are said to be velocity detectors and acceleration detectors [11], respectively.

The prototype system produced 0.64 gf as a total force. Even if the total force is completely converged on a 1mm diameter spot, the force is considered to be a little weak for continuous pressure sensation, though it is sufficient for inducing vibratory sensation. As we show in Fig.13, PZT transducer has a saturation point when the input electricity is increased. In order to produce sufficient force, the total area of the radiating surface should be about 10 times larger than the prototype system.

Acknowledgement

This work is partly supported by JSPS Research Fellowships for Young Scientists.

References

[1] H. Kajimoto, N. Kawakami, T. Maeda and S. Tachi: “Tactile Feeling Display using Functional Electrical Stimulation,” Proc. 1999 ICAT, 1999.

[2] Y. Ikei, K. Wakamatsu and S. Fukuda, “Image Data Transformation for Tactile Texture Display,” Proc.VRAIS ’98, pp.51-58, 1998.

[3] G. Moy, C. Wagner, R.S. Fearing, “A Compliant Tactile Display for Teletaction,” Proc. IEEE Int Conf. Robotics and Automation, pp. 3409-3415, 2000.

[4] M. Konyo, S. Tadokoro, T. Takamori, K. Oguro, "Artificial Tactile Feeling Display Using Soft Gel Actuators", Proc. 2000 IEEE Int. Conf. on Robotics and Automation, pp.3416-3421, April, 2000.

[5] J. Pasquero and V. Hayward: “STReSS: A Practical Tactile Display System with One Millimeter,” Proc. of Eurohaptics 2003, 2003.

[6] D.Dalecki, S.Z.Child, C.H.Raeman and E.Carlstensen: Tactile perception of ultrasound, Journal of acoustical society of America, vol.97,(5), Pt.1, pp.3165-3170, May 1995.

[7] T.Iwamoto, T.maeda, H.Shinoda, "Focused Ultrasound for Tactile Feeling Display" in The Eleventh International Conference on Artificial reality and Telexistence (ICAT'2001), 2001.

[8] Friedman RM, Khalsa PS, Greenquist KW, LaMotte RH, “Neural coding of the location and direction of a moving object by a spatially distributed population of mechanoreceptors”, Journal of Neuroscience 22 (21): pp. 9556-9566, Nov, 2002

[9] W.Lee and S.W.Smith, “Intracardiac Catheter 2-D Arrays on a silicon Substrate”, IEEE ultrasonics ferroelectrics, and frequency control, vol.49, No.4, pp.415-425, 2002

[10] A.B.Vallbo and R.S.Johansson, ”Properties of Cutaneous Mechanoreceptors in the Human Hand Related to Touch Sensation”, Human Neurobiol. vol.3, pp3-14, 1984

[11] R.F Schmidt, ”Fundamentals of sensory Physiology”, Springer-Verlag, 1986